Applied Catalysis B: Environmental 331 (2023) 122705

Contents lists available at ScienceDirect

Applied Catalysis B: Environmental

journal homepage: www.elsevier.com/locate/apcatb

Maximizing the hydrothermal stability of Cu-LTA for NH_3-SCR by control of Cu content and location

Jinhan Lin [a,b], Xueyang Hu [a,b,c], Yingjie Li [a,b,c], Wenpo Shan [a,b,*], Xuechao Tan [d], Hong He [a,c,e,*]

[a] Center for Excellence in Regional Atmospheric Environment and Key Laboratory of Urban Pollutant Conversion, Institute of Urban Environment, Chinese Academy of Science, Xiamen 361021, China
[b] Zhejiang Key Laboratory of Urban Environmental Processes and Pollution Control, Ningbo Urban Environment Observation and Research Station, Institute of Urban Environment, Chinese Academy of Sciences, Ningbo 315800, China
[c] University of Chinese Academy of Sciences, Beijing 100049, China
[d] Center for Ordered Nanoporous Materials Synthesis, Division of Environmental Science and Engineering, POSTECH, Pohang 37673, South Korea
[e] State Key Joint Laboratory of Environment Simulation and Pollution Control, Research Center for Eco-Environmental Sciences, Chinese Academy of Sciences, Beijing 100085, China

ARTICLE INFO

Keywords:
Cu-LTA
Cu content
Cu species
Hydrothermal stability
NH_3-SCR

ABSTRACT

Hydrothermal stability is crucial for the application of NO_x emission control catalysts on diesel vehicles. In this study, the influences of Cu content and Cu species on the catalytic performance and hydrothermal stability of copper-exchanged LTA (Cu-LTA) zeolite catalysts for the selective catalytic reduction of NO_x with NH_3 (NH_3-SCR) have been systematically investigated. The Cu-LTA(n)−0.41 catalyst with the maximum amount and ratio of Cu^{2+}-2Z species in Cu-LTA, with Cu/Al = 0.41 and Si/Al = 16, was produced by full occupation of Al pairs in the single 6-rings (*s6rs*) with Cu^{2+} ions. This catalyst showed higher deNO_x activity after hydrothermal aging under extremely harsh conditions of 920 °C for 24 h than any of the other catalysts. The results suggest that maximizing the amount of Cu^{2+}-2Z species and diminishing the formation of comparatively vulnerable $[Cu(OH)]^+$-Z species in the high-silica LTA zeolite is an effective strategy for developing hydrothermally stable NH_3-SCR catalysts.

1. Introduction

Nitrogen oxides (NO_x, including NO and NO_2) are among the primary air pollutants and can cause haze, photochemical smog, and acid rain [1–3]. In China, the NO_x from diesel vehicles accounts for approximately 90% of that emitted from automobiles, and NO_x emissions from diesel engines used as non-mobile power sources are comparable to those from road vehicles [4]. Selective catalytic reduction of NO_x with ammonia (NH_3-SCR) over Cu-exchanged small-pore zeolite catalysts is considered one of the most efficient techniques for diesel-powered lean combustion vehicles [5–7]. NH_3-SCR catalysts in the diesel after-treatment system are usually located after the diesel particle filter (DPF), which needs to be regenerated periodically at high temperatures, sometimes higher than 800 °C. Unfortunately, the commercial Cu-SSZ-13 catalyst suffers from severe deactivation under the conditions of hydrothermal aging at ≥ 800 °C for tens of hours [8,9]. Besides hydrothermal stability, the NH_3-SCR catalysts should also have good resistance against alkali metals, phosphorus, and sulfur. Extensive research efforts have been made to improve the deNO_x efficiency and poisoning tolerance [10–13]. Therefore, there is still market demand for a more robust metal-exchanged zeolite SCR catalyst [14–16].

Previous reports showed that Cu-exchanged LTA (Si/Al = 16, 23) can maintain high deNO_x activity and structural integrity after hydrothermal aging treatment at 900 °C, outperforming the current commercial Cu-SSZ-13 catalyst [17–21]. It is widely accepted that Cu^{2+} ions balanced by two Al atoms in the *s6r* (Cu^{2+}-2Z) are more stable than $[Cu(OH)]^+$ balanced by one single Al atom ($[Cu(OH)]^+$-Z), where Z represents the single negative charge created by Al substitution in the zeolite framework [22–25]. In addition, it is concluded that $[Cu(OH)]^+$-Z species are more easily converted to CuO_x during hydrothermal aging and more vulnerable to SO_2 and P poisoning than Cu^{2+}-2Z species [26,27]. To enhance the hydrothermal stability of Cu-exchanged zeolite catalysts, many researchers have sought to increase the amount/ratio of Cu^{2+}-2Z [25,28–30]. Chen and co-workers reported that more

* Corresponding authors at: Center for Excellence in Regional Atmospheric Environment and Key Laboratory of Urban Pollutant Conversion, Institute of Urban Environment, Chinese Academy of Science, Xiamen 361021, China.
E-mail addresses: wpshan@iue.ac.cn (W. Shan), honghe@rcees.ac.cn (H. He).

https://doi.org/10.1016/j.apcatb.2023.122705
Received 19 January 2023; Received in revised form 24 March 2023; Accepted 27 March 2023
Available online 28 March 2023

hydrothermally stable Cu^{2+}-2Z could suppress the loss of active Cu ions and dealumination during hydrothermal aging, and thus the hydrothermal stability of Cu-SSZ-13 was improved remarkably [29]. The introduction of Y can induce more Cu^{2+}-2Z to form in Cu-SSZ-39, and Y-modified Cu-SSZ-39 showed comparable $deNO_x$ activity after hydrothermal aging at 900 °C for 10 h [30]. Therefore, an increase in the amount and ratio of Cu^{2+}-2Z can improve the $deNO_x$ activity and hydrothermal stability of Cu-LTA. Because of the various Cu complexes in Cu solutions, the location of Cu^{2+} ions can be affected by the use of different Cu precursors [31,32]. Our previous work investigated the influence of Cu precursors on the catalytic properties and hydrothermal stabilities of Cu-LTA catalysts, and it was found that the excellent hydrothermal stability of Cu-LTA prepared using Cu nitrate originated from the stability of Cu^{2+}-2Z species [21]. However, the inadequate content of Cu in the Cu-LTA-16 (Si/Al = 16) catalyst, with Cu/Al = 0.18, leads to low $deNO_x$ activity at low temperature. Thus, the vacant Al pairs in the *s6rs* need to be occupied by more Cu^{2+}-2Z species through increasing the Cu content and precise control of its location.

In view of the fact that the $deNO_x$ activity and hydrothermal stability of Cu-exchanged zeolites in the NH_3-SCR reaction largely depend on the Cu content [17,33–35], we herein prepared Cu-LTA catalysts using Cu nitrate with various Cu loadings (1.7–2.4 wt%) via the liquid-phase ion exchange (IE) method and hydrothermally aged them at 920 °C for 24 h to investigate the effect of Cu content and its location (Cu species). It is necessary to specify that the Cu exchange level is defined as $\frac{\text{mole Cu}}{\text{mole Al}} \times 200\%$ [23,36]. When the ratio of Cu/Al = 0.5, the corresponding Cu-exchange level reaches 100%, which is so-called fully Cu-exchanged. In this work, it was shown that control of the ratio of Cu/Al in Cu-LTA to equal to the ratio of Co/Al in Co-exchanged LTA-16 with the maximum ion exchange of Co^{2+} ions can be achieved, and that the formation of comparatively unstable $[Cu(OH)]^+$-Z species can be suppressed. It is worth noting that the Cu-LTA(n)−0.44 prepared using Cu nitrate as Cu precursor, with a Cu/Al ratio of 0.44, required four cycles of the IE process to reach a high Cu-exchange level, and it is hard to reach higher Cu-exchange levels by the IE method with Cu nitrate. In our previous study, a Cu-LTA(a)−0.48 catalyst, prepared using Cu acetate with a Cu/Al ratio of 0.48, was proved to be efficient for NH_3-SCR; however, in this catalyst a considerable amount of unstable $[Cu(OH)]^+$-Z species existed, which led to severe deactivation when the hydrothermal aging treatment was extended from 12 h to 24 h [18]. To elucidate the importance of Cu content and location, the fully Cu-exchanged LTA catalyst (Cu/Al = 0.5) using Cu acetate as Cu precursor was also synthesized for comparison. The $deNO_x$ activities of the prepared Cu-LTA catalysts were evaluated, and the physicochemical properties of the catalysts were systematically investigated via XRD, N_2 adsorption and desorption, ICP, H_2-TPR, EPR, SEM, UV–vis, and *in situ* DRIFTS.

2. Experimental

2.1. Catalyst preparation

LTA zeolite with Si/Al = 16 was hydrothermally synthesized according to the procedure previously reported [18–20]. Ammonium-type LTA zeolite (NH_4-LTA) was formed through ion-exchange of proton-type LTA zeolite (H-LTA) twice with 1 M NH_4Cl solution (2.0 g of solid per 100 mL of solution). Cu-LTA catalysts with various Cu contents were obtained by the IE method using 0.01–0.1 M of either Cu acetate ($Cu(CH_3COO)_2{\cdot}1.0\ H_2O$, 97.0%, Aldrich), or Cu nitrate ($Cu(NO_3)_2{\cdot}2.5\ H_2O$, 98.0%, Aldrich) solutions. The time and number of ion exchange cycles were properly adjusted. The solids were collected by filtration, washed with deionized water, dried overnight at 110 °C, and finally calcined in air at 550 °C for 8 h. The catalysts obtained were finally denoted as Cu-LTA(*x*)-y, where *x* and y represent the type of Cu precursor (a for Cu acetate; n for Cu nitrate) and the Cu/Al ratio, respectively. It is worth noting that the prepared Cu-LTA(n)−0.44 required four cycles of the IE process to reach a high Cu-exchange level, and it is hard to reach higher Cu-exchange levels by the IE method with Cu nitrate.

The hydrothermal aging treatment was performed in air containing 10% H_2O at 850–920 °C for 24 h. Cobalt-exchanged LTA (Co-LTA-16) was prepared by ion-exchanging NH_4-LTA with 1.0 M cobalt nitrate solution ($Co(NO_3)_2{\cdot}6\ H_2O$, 98.0%, Aldrich) at 80 °C for 12 h. In order to maximize the amount of exchanged Co^{2+}, this procedure was repeated three times. Subsequently, the resulting solid was calcined in air at 550 °C for 8 h [25].

2.2. Characterization

Powder X-ray diffraction (XRD) measurements in the 2θ range of 5–60° were obtained using a PANalytical Empyrean diffractometer with Cu K_α radiation. The BET surface areas of the catalysts were determined from nitrogen adsorption/desorption isotherms by a ASAP2460 Analyzer. Prior to the measurement, the sample was degassed in vacuum at 300 °C for 2 h to remove adsorbed water. UV–vis spectra were collected using a PerkinElmer Lambda 950 UV–vis spectrophotometer.

The H_2 temperature-programmed reduction (H_2-TPR) experiments were conducted on a chemisorption analyzer (Micromeritics AutoChem II 2920). Typically, 100 mg of catalyst was pretreated under 5% O_2/He at 500 °C for 1 h and then cooled down to 50 °C. Finally, the sample was heated to 800 °C in a 5% H_2/Ar under a flow rate of 50 mL·min^{-1} at a heating rate of 10 °C·min^{-1}.

The *in situ* diffuse reflectance infrared Fourier transform spectroscopy (*in situ* DRIFTS) experiments were carried out on an FTIR spectrometer (Nicolet IS50) equipped with an MCT/A detector, and the obtained spectra were converted using the Kubelka-Munk function. Prior to each experiment, the sample was pretreated in 100 mL·min^{-1} of 10% O_2/N_2 at 500 °C for 1 h to remove impurities. The background spectra were collected after cooling to 200 °C and automatically subtracted from the sample spectra. For the NH_3 adsorption, the Cu-LTA catalysts were exposed to NH_3 (500 ppm NH_3, 10% O_2, and N_2 balance) at 200 °C until saturation, where DRIFT spectra were continuously recorded during the adsorption process.

The morphologies of Cu-LTA catalysts were determined by field-emission scanning electron microscopy (SEM, ZEISS SIGMA 500). Prior to imaging, the samples were fixed on conductive carbon tape. Inductively coupled plasma (ICP) was used to analyze the Cu, Al, and Si contents of the catalysts on an ICP-OES 730 inductively coupled plasma spectrometer, and the samples were dissolved in strong acid. The TEM images were obtained using a JEOL JEM-F200 transmission electron microscope operating at 200 kV. Prior to measurement, the samples were suspended in ethanol and then dried on a holey carbon film Cu grid. The EPR spectra were collected on a Bruker A300 spectrometer. The EPR spectrometer settings were as follows: center field 3200 G; sweep width 2000 G; microwave frequency 9.65 GHz; modulation frequency 100 kHz; power 19.57 mW. Solid state 27Al MAS NMR spectra were collected on a JNM-ECZ600R spectrometer operating at the spectral frequency of 156 MHz. A relaxation delay of 5 s for Al was applied to collect single-pulse spectra. All measurements were carried out at room temperature.

2.3. Activity tests

The $deNO_x$ activity of the as-prepared Cu-LTA catalysts was evaluated in a fixed-bed reactor in the temperature range of 150–600 °C, with a gas hourly space velocity (GHSV) of 100,000 h^{-1}. The composition of the feed gas was 500 ppm NH_3, 500 ppm NO, 5% O_2, 10% H_2O, and N_2 balance. 0.3 mL of the catalysts (40–60 mesh) was loaded in a quartz tube reactor between two quartz wool plugs, and the total gas flow rate was controlled at 500 mL·min^{-1}. The content of feed and outlet gases was continuously analyzed by a gas analyzer (Antaris IGS, Thermo Fisher) equipped with a heated gas cell. The NO_x conversion and N_2

selectivity were calculated based on the equations below, respectively:

$$NO_x \text{ conversion} = \left(\frac{[NO_x]_{in} - [NO_x]_{out}}{[NO_x]_{in}}\right) \times 100\% \quad (1)$$

$$N_2 \text{ selectivity} = \left(1 - \frac{2[N_2O]_{out}}{[NO_x]_{in} - [NO_x]_{out} + [NH_3]_{in} - [NH_3]_{out}}\right) \times 100\% \quad (2)$$

3. Results and discussion

3.1. Reaction results

Fig. 1 depicts the NO_x conversion as a function of temperature over the fresh and hydrothermally aged Cu-LTA catalysts prepared using different Cu precursors with different Cu loadings. The deNO_x activities of the fresh Cu-LTA catalysts in the range of 150–300 °C became higher in the order Cu-LTA(n)−0.32 < Cu-LTA(n)−0.41 < Cu-LTA(n)−0.44 < Cu-LTA(a)−0.50, which is in line with their Cu contents (Table 1). However, the Cu-LTA catalyst with higher Cu content presented lower deNO_x activity at temperatures above 500 °C. After hydrothermal aging at 920 °C for 24 h, all of the Cu-LTA catalysts prepared using Cu nitrate showed excellent deNO_x activity and hydrothermal stability compared with Cu-LTA(a)−0.50. Most impressively, extraordinarily high conversion levels (NO_x > 90%) could be maintained for the Cu-LTA(n)−0.41 catalyst over the entire active temperature window of 250–500 °C. We had found that the fully Cu-exchanged LTA catalyst (Cu/Al = 0.48) prepared using copper acetate lost its deNO_x activity after treatment at 900 °C for 24 h in air containing 10% water [18]. Thus, it is not surprising that the hydrothermally aged Cu-LTA(a)−0.50 catalyst almost completely lost its activity under such severe conditions. In the previous study, it was found that the Cu-LTA catalyst with Cu/Al = 0.31 prepared using Cu nitrate and the IE method exhibited excellent hydrothermal stability [21]. However, its low-temperature (< 300 °C) activity was poor due to the low Cu loading (1.8 wt%). Thus, the performance of the aged Cu-LTA catalysts demonstrated that both the

Table 1
The physical data of Cu-LTA catalysts investigated in this work.

Catalysts	Cu (Co) loading (wt%)[a]	Cu (Co)/Al	BET surface area ($m^2\ g^{-1}$)[b]	
			Fresh	Aged
Cu-LTA(n)−0.32	1.7	0.31	754	713[c]
Cu-LTA(n)−0.41	2.1	0.41	750	521[c]
Cu-LTA(n)−0.44	2.4	0.44	749	262[c]
Cu-LTA(a)−0.50	2.8	0.50	746	59[c]
Cu-LTA(n)−0.41	2.1	0.41	750	750[d]
Cu-LTA(n)−0.41	2.1	0.41	750	731[e]
H-LTA	-	-	760	-
Co-LTA	2.0	0.41	-	-

[a] Determined by elemental analysis of ICP.
[b] Calculated from N_2 adsorption data.
[c] hydrothermal aging at 920 °C for 24 h.
[d] hydrothermal aging at 850 °C for 24 h.
[e] hydrothermal aging at 900 °C for 24 h.

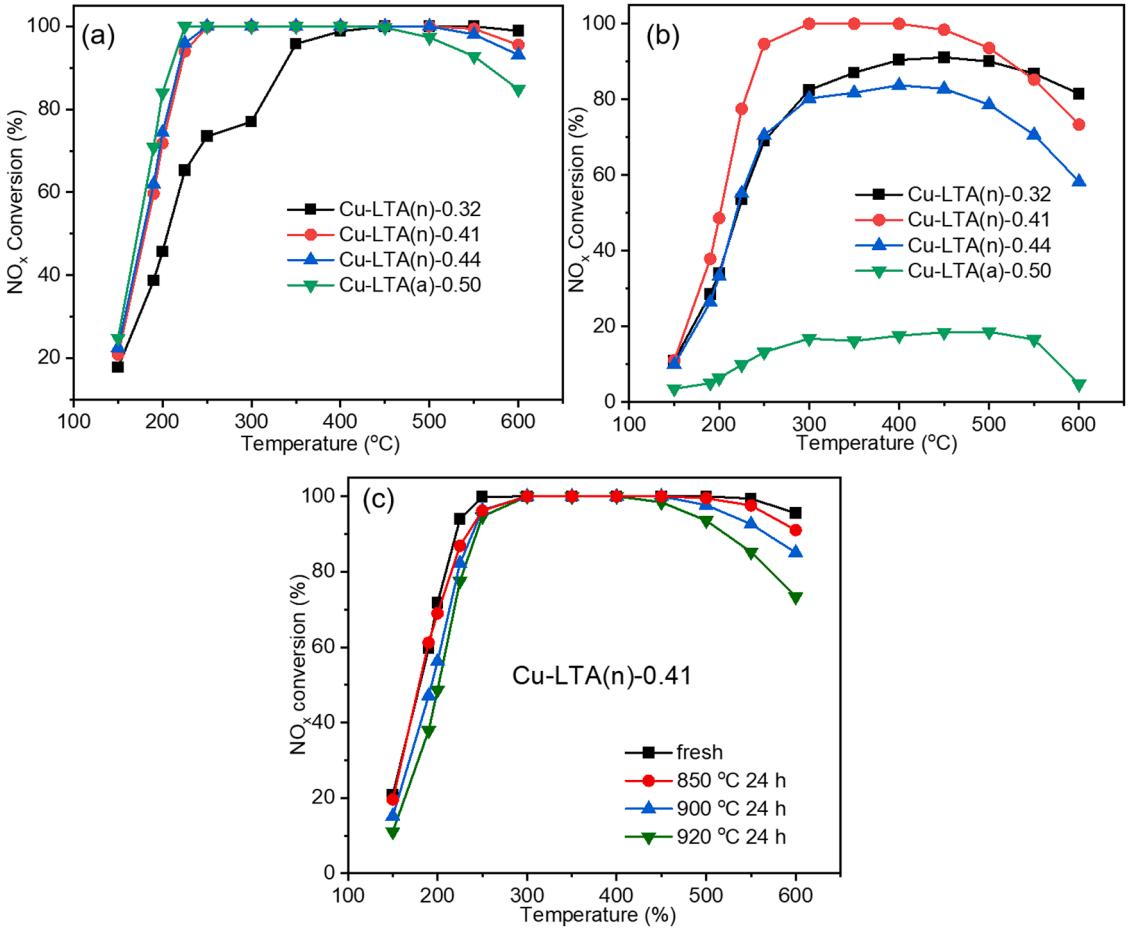

Fig. 1. NO_x conversion as a function of temperature over the (a) fresh and (b) 920 °C-aged Cu-LTA catalysts prepared using different Cu precursors with different Cu loadings: Cu-LTA(n)−0.32 (■), Cu-LTA(n)−0.41 (●), and Cu-LTA(n)−0.44 (▲), and Cu-LTA(a)−0.50 (▼). The feed gas contained 500 ppm NH_3, 500 ppm NO, 5% O_2, 10% H_2O, and N_2 balance, at a GHSV of 100,000 h^{-1}. Hydrothermal aging was carried out in air containing 10% H_2O at 920 °C for 24 h. (c) NO_x conversion profiles for Cu-LTA(n)−0.41 catalyst hydrothermally aged at various temperatures.

selection of Cu precursors and the Cu loading have significant effects on the hydrothermal stability of Cu-LTA catalysts. The N_2 selectivity of fresh and 920 °C-aged Cu-LTA catalysts is shown in Fig. S1. For the fresh Cu-LTA catalysts, the N_2 selectivity was nearly 100%. However, after hydrothermal aging treatment, the N_2 selectivity decreased in the high-temperature region (400–600 °C) since the Brønsted acid sites were destroyed during the hydrothermal aging treatment, and the nonselective oxidation of NH_3 occurred [37]. To further investigate the potential application of the Cu-LTA(n)−0.41 catalyst for other vehicles whose exhausts contain more steam at high temperature, such as H_2-fueled engine vehicles, the Cu-LTA(n)−0.41 catalyst was hydrothermally aged at 850 °C for 24 h in air containing 20% H_2O (Fig. S2). Surprisingly, the active temperature window (NO_x > 90%) of the Cu-LTA(n)−0.41 catalyst was still maintained in the range of 250–600 °C.

It is well known that isolated Cu^{2+} ions (Cu^{2+}-2Z and $[Cu(OH)]^+$-Z) in Cu-exchanged zeolites are the active sites for NH_3-SCR [7]. Moreover, Cu^{2+}-2Z species are more stable than $[Cu(OH)]^+$-Z species under hydrothermal treatment conditions [22,25]. During the IE process, Cu ions coordinate to all available Al pairs as Cu^{2+}-2Z before occupying single-atom Al sites as $[Cu(OH)]^+$-Z [38]. It is noteworthy that the "monovalent" Cu^{2+} species ($[Cu\text{-}CH_3COO]^+$ or $[Cu\text{-}OH]^+$) ion-exchanged in NH_4-LTA only exist in copper acetate solution [31,32], while the Cu^{2+} species in Cu nitrate solution are present in the form of aquo-complexes ($[Cu(H_2O)_6]^{2+}$). Because the single-atom Al sites can readily exchange with "monovalent" Cu^{2+} species in the Cu acetate solution, the Cu-LTA(a) catalyst can easily reach complete (Cu/Al = 0.5) or over-exchanged (Cu/Al > 0.5) levels of Cu ions, while it is hard to reach high Cu-exchange levels for Cu-LTA(n) catalysts in the Cu nitrate solution. Although the high Cu content results in enhanced $deNO_x$ activity for the Cu-LTA(a) catalyst in the low-temperature region, the higher concentration of $[Cu(OH)]^+$-Z species can easily agglomerate to CuO_x during hydrothermal aging [22], which would cause low hydrothermal stability, as observed for Cu-LTA(a). Since Cu nitrate solution only contains $[Cu(H_2O)_6]^{2+}$, Cu^{2+} ions have difficulty occupying the single-Al sites before all of the Al pairs are occupied [38]. Therefore, theoretically, it is feasible to synthesize Cu-LTA catalysts with fully-Cu-occupied Al pairs and no Cu-occupied single-Al sites by using Cu nitrate solution.

The Cu-LTA catalyst with Si/Al = 16 has superior hydrothermal stability owing to the Cu^{2+} ions being located in the *s6r* centers only [18]. Thus, it is quite meaningful to completely Cu-exchange all Al pairs in the LTA with Si/Al = 16. In order to measure the amount of Al pairs in LTA zeolite employed in this work, the cobalt content of cobalt-exchanged LTA with the maximum achievable ion exchange of Co^{2+} ions was analyzed by ICP, since Co^{2+} ions are exchanged at Al pairs to form Co^{2+}-2Z [39]. To better understand this work, the effects of Cu contents on the locations of Cu species are illustrated in Scheme 1. The obtained ratio of Co/Al = 0.41 manifests that almost all of the Al pairs in LTA were exchanged by Cu^{2+} ions since the Al pairs were preferentially occupied in the Cu nitrate solution. Thus, the amount of Cu^{2+}-2Z species reached a maximum value in the Cu-LTA(n)−0.41 catalyst [31,38]. In the case of the aged Cu-LTA(n)−0.44 catalyst, the excess Cu^{2+} ions would form as $[Cu(OH)]^+$-Z species, which will be easier to transform to CuO_x, leading to the loss of $deNO_x$ activity and the collapse of the zeolite structure during hydrothermal aging treatment. Furthermore, highly mobile CuO_x will agglomerate to form CuO_x clusters and cause severe

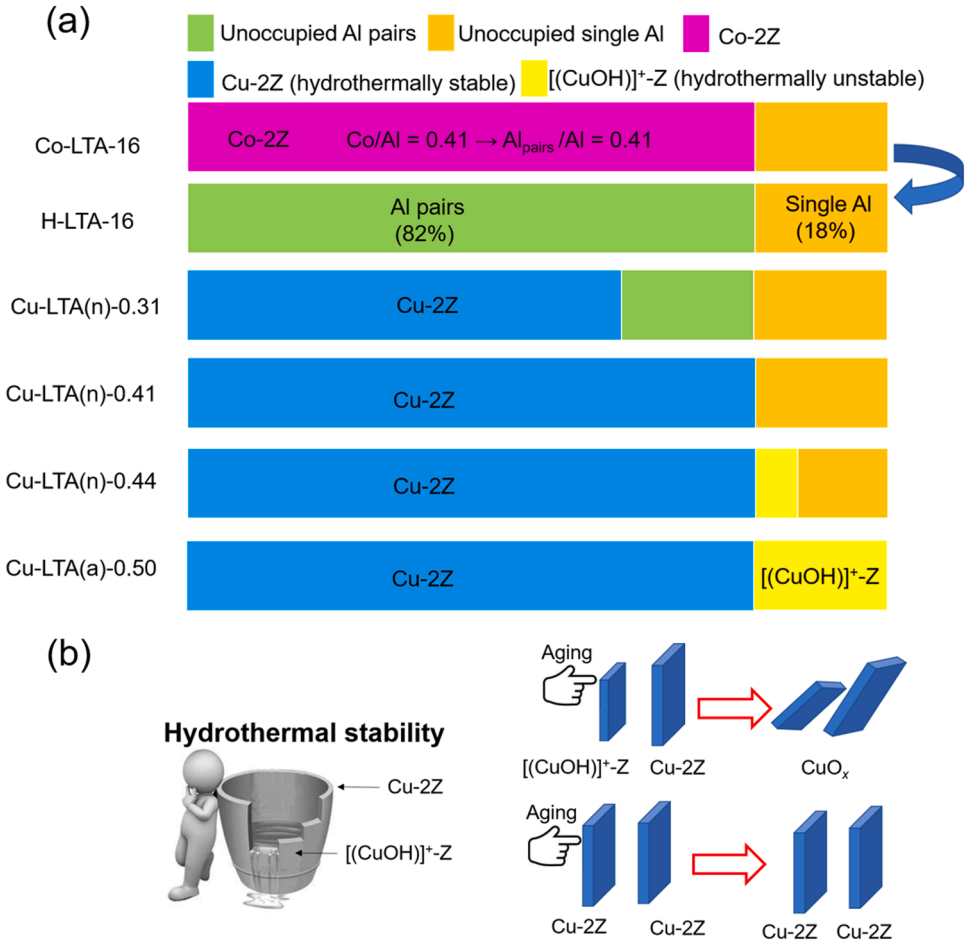

Scheme 1. Illustration of (a) the preparation process for controlling the Cu contents and (b) the effect of different Cu species on the hydrothermal stability of Cu-LTA catalysts.

structural destruction due to its migration under hydrothermal aging conditions [22]. In Table 1, the surface areas of fresh and aged Cu-LTA catalysts are presented. After hydrothermal aging at 920 °C for 24 h, it is impressive that the surface area of Cu-LTA(n)−0.32 remained as high as 710 $m^2 \cdot g^{-1}$, which illustrates the incredible stability of Cu-LTA. On the other hand, from the drop in surface area of the Cu-LTA(a)−0.50 catalyst from 750 $m^2 \cdot g^{-1}$ to 60 $m^2 \cdot g^{-1}$ one can conclude that the zeolite structure collapsed. Combined with the deNO_x activities of fresh and aged Cu-LTA catalysts employed in this work, what can be inferred is that Cu loading and location are both vital for hydrothermal stability.

To further investigate the hydrothermal stability of the Cu-LTA(n)−0.41 catalyst, various hydrothermal aging temperatures were employed. The difference in the deNO_x activity between the fresh and 850 °C-aged Cu-LTA(n)−0.41 is relatively small. The activity temperature window (NO_x > 90%) of the Cu-LTA(n)−0.41 catalyst can be maintained in the range of 250–550 °C after hydrothermal aging at 900 °C for 24 h. In order to investigate the durability of the Cu-LTA(n)−0.41 catalyst, the Cu-LTA(n)−0.41 catalyst was hydrothermally aged at various temperatures. There were no significant differences in the deNO_x activities of fresh and 850 °C-aged Cu-LTA(n)−0.41 catalyst in the temperature range we used in this work, which is in good agreement with the surface area results of the catalysts. The results demonstrate that the Cu-LTA(n)−0.41 catalyst is suitable for practical application.

3.2. Characterization results

The powder XRD patterns of the fresh and 920 °C-aged Cu-LTA catalysts prepared in this study are shown in Fig. 2. Comparison of the powder XRD patterns of the fresh Cu-LTA catalysts revealed no noticeable differences in the positions or relative intensities of all the X-ray peaks. However, after hydrothermal aging at 920 °C for 24 h, a noticeable decrease in XRD intensity occurred for the Cu-LTA(a)−0.50 catalyst. In particular, a broad halo at about 22 ° was observed, which is a representative feature of amorphous silica phases [40,41]. This type of amorphous phase is usually detected in high-temperature hydrothermally aged Cu-exchanged zeolite catalysts, such as Cu-SSZ-13, which indicates collapse of the zeolite, dealumination, and severe deactivation of the catalysts [8,42,43]. These results reveal that the destruction of the Cu-LTA(a)−0.50 catalyst appears to be the main reason for its deactivation upon hydrothermal aging treatment, indicating the poor stability of Cu-LTA(a)−0.50 catalyst compared with other Cu-LTA catalysts prepared in this work. However, no diffraction peaks attributed to CuO_x can be observed for the aged Cu-LTA(a)−0.50 catalyst, implying that either no CuO_x has been formed or that the particle size of CuO_x is too small to be detected by XRD. The XRD patterns and BET results are consistent with the deNO_x activities in Fig. 1, which demonstrates that the Cu-LTA(n)−0.41 catalyst maintained high surface area and an intact zeolite structure to support the Cu^{2+}-2Z species to achieve high deNO_x activity after hydrothermal aging treatment.

To identify the different types of Cu sites in Cu-LTA catalysts, *in situ* DRIFTS of NH_3 adsorption was performed to distinguish the Cu^{2+}-2Z species and $[Cu(OH)]^+$-Z species, which can be observed as negatively perturbed T-O-T vibration IR signals, since framework O ligands are replaced by NH_3 molecules to interact with Cu [44]. As shown in Fig. 3, two well-resolved negative bands centered at around 960 cm^{-1} and 920 cm^{-1} can be clearly observed in the spectrum of the Cu-LTA(a)−0.50 catalyst, which are attributed to perturbation of the T-O-T vibration in the LTA framework by the $[Cu(OH)]^+$-Z and Cu^{2+}-2Z species in *s6rs*, respectively. It is evident that no detectable band around 960 cm^{-1} can be found for the Cu-LTA(n)−0.32, Cu-LTA(n)−0.41, or Cu-LTA(n)−0.44 catalysts, indicating that the amounts of $[Cu(OH)]^+$-Z species in those catalysts are relatively low. On the other hand, excess $[Cu(OH)]^+$-Z species in the Cu-LTA(a)−0.50 catalyst lead to considerably poorer hydrothermal stability than that of the other three Cu-LTA catalysts prepared using Cu nitrate.

It has been reported that the Cu^{2+}-2Z species in Cu-SSZ-13 can be maintained under severe hydrothermal aging conditions (900 °C for 2 h), while the $[Cu(OH)]^+$-Z species gradually agglomerated to form CuO_x clusters [23]. Moreover, the ~900 cm^{-1} band assigned to the Cu^{2+}-2Z species in fresh Cu-SSZ-13 shifted to ~920 cm^{-1} after hydrothermal aging treatment, but the intensity remained the same [23]. During the hydrothermal aging treatment, the Cu^{2+} ions will migrate to

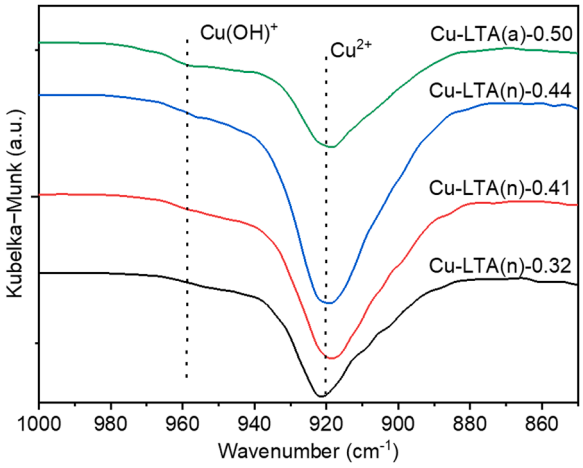

Fig. 3. DRIFT spectra of T-O-T vibrational region perturbed by NH_3 adsorption over fresh Cu-LTA(n)−0.32, Cu-LTA(n)−0.41, Cu-LTA(n)−0.44, and Cu-LTA(a)−0.50 (from bottom to top).

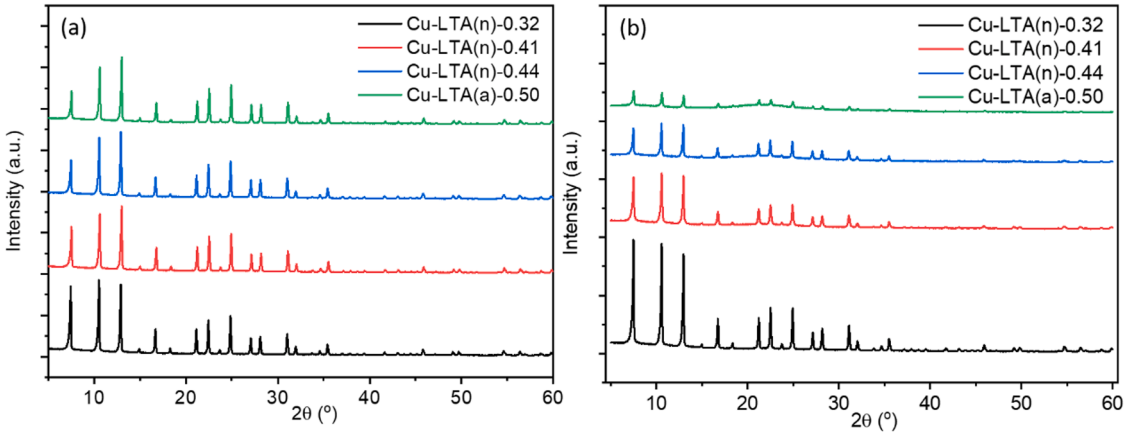

Fig. 2. Powder XRD patterns of the (a) fresh and (b) 920 °C-aged Cu-LTA catalysts.

more-stable Al pair sites and form Cu^{2+}-2Z species. This is the reason why the "degreening" process is usually used for pretreatment before SCR testing [44]. The combination of our results and those in the literature mentioned above convincingly demonstrates that having the maximum amount of Cu^{2+}-2Z species gives the Cu-LTA(n)−0.41 catalyst excellent deNO_x activity and hydrothermal stability. It is also noteworthy that the small excess of $[Cu(OH)]^+$-Z species in the Cu-LTA(n)−0.44 catalyst led to a drop in the surface area and deNO_x activity after hydrothermal aging treatment; furthermore, the considerable excess of $[Cu(OH)]^+$-Z species in the Cu-LTA(a)−0.50 catalyst led to a collapse in the zeolite structure and a significant loss of activity. Adjusting or increasing the Al pairs to provide more Cu^{2+}-2Z species has been reported to be an effective strategy for enhancing the hydrothermal stability of Cu-SSZ-13 [4,25,29]. Because the percentage of Al pairs in LTA with Si/Al = 16 is quite high (about 82%), this work mainly focused on control of the Cu content and location, instead of further improving the ratio of Al pairs. If there are no $[Cu(OH)]^+$-Z species in the Cu-LTA(n)−0.41 catalyst, all Cu^{2+} ions will form Cu^{2+}-2Z species, which are hydrothermally stable under severe conditions. Thus, suppression of the formation of comparatively less-stable $[Cu(OH)]^+$-Z species during the synthesis of Cu-LTA(n)−0.41 by IE with Cu nitrate solution is effective for enhancing the catalytic performance of Cu-LTA catalysts.

As shown in Fig. 4, UV–vis spectroscopy was used for the detection of Cu species in fresh and 920 °C-aged Cu-LTA catalysts prepared in this work. The spectra of all fresh Cu-LTA catalysts are characterized by the $O^{2-} \rightarrow Cu^{2+}$ (lattice oxygen to isolated Cu^+/Cu^{2+} ions) charge-transfer transition band at ~220 nm and the d-d transition band of Cu^{2+} (CuO surrounded by oxygen) in octahedral coordination at ~750 nm [45–47], indicating that the dominant Cu species in the fresh Cu-LTA catalysts are isolated Cu^{2+} ions. After hydrothermal aging treatment at 920 °C for 24 h, a charge-transfer band is observed, suggesting the transformation of Cu^{2+} ions to oligonuclear $[Cu\text{-}O\text{-}Cu]_n$ (280–330 nm) and/or crystalline CuO_x (330–420 nm) species [45,46]. We also note that the aged Cu-LTA(a)−0.50 catalyst gives a broader $O^{2-} \rightarrow Cu^{2+}$ charge-transfer transition band than the other three aged Cu-LTA catalysts prepared using Cu nitrate. This fact indicates that more transformation of isolated Cu^{2+} ions to other forms of Cu occurred in the Cu-LTA(a)−0.50 catalyst, which leads to the severe loss of deNO_x activity and structural stability.

To further investigate the state of the Cu species in the Cu-LTA catalysts prepared in this work, H_2-TPR was carried out to reveal the differences in the binding energies with the framework based on differences in reducibility. The H_2-TPR profiles of the fresh and 920 °C-aged Cu-LTA catalysts prepared here are illustrated in Fig. 5. For the fresh catalysts, two peaks centered at ~250 °C and 340 °C were observed, indicating that two types of Cu species existed. The intensity of the reduction peaks increased with the increase in Cu loading, which is in line with the ICP results. According to the literature, the reduction peaks at ~250 °C and ~340 °C were assigned to $[Cu(OH)]^+$-Z and Cu^{2+}-2Z species, respectively, because the binding energy of $[Cu(OH)]^+$-Z with the framework is lower than that of Cu^{2+}-2Z [17,24,48]. The populations of different Cu species were calculated based on the deconvolution of H_2-TPR profiles and listed in Table 2. Both $[Cu(OH)]^+$-Z and Cu^{2+}-2Z species existed in the fresh Cu-LTA catalysts. Moreover, the percentage of $[Cu(OH)]^+$-Z species in the Cu-LTA(a)−0.50 catalyst is higher than that of the Cu-LTA(n) catalysts, which is in good agreement with the results of DRIFTS. It is interesting that the percentage of Cu^{2+}-2Z species in the Cu-LTA(n)−0.32 catalyst increased from 92% to 98% after hydrothermal aging treatment due to the conversion of $[Cu(OH)]^+$-Z to Cu^{2+}-2Z species.

To identify the changes in Cu species in Cu-LTA catalysts during hydrothermal aging treatment, the H_2-TPR profiles of the 920 °C-aged forms of Cu-LTA catalysts were deconvoluted. The profile of the Cu-LTA(a)−0.50 catalyst could be deconvoluted into four main contributions. These peaks centered at around 225, 332, 425, and 526 °C were assigned to highly dispersed CuO_x species, bulk CuO_x species, Cu^{2+} ions located in less reducible sites, and $CuAl_2O_4$, respectively [45,49]. Interestingly, it was found that the reduction peaks of CuO_x species and $CuAl_2O_4$ are in good agreement with those of a CuO/Al_2O_3 sample calcined at 900 °C [49]. For the aged forms of Cu-LTA(n)−0.32 and Cu-LTA(n)−0.41 catalysts, although CuO_x species can be observed, most Cu species are still maintained as Cu^{2+} ions. Notably, no noticeable reduction peak for $CuAl_2O_4$ can be found, indicating that the Al species still existed in the framework and no appreciable dealumination occurred. The combined XRD, BET, and H_2-TPR results suggest that the transformation of Cu^{2+} ions to CuO_x and the collapse of the LTA structure are the main reasons for the deactivation of the Cu-LTA(a)−0.50 catalyst. It is also noteworthy that the aged Cu-LTA(n)−0.44 catalyst contains much more CuO_x and $CuAl_2O_4$ than the aged Cu-LTA(n)−0.41 catalyst, since excess $[Cu(OH)]^+$-Z exists beyond the maximum amount of available Al pairs in LTA-16.

Because Cu^{2+}-2Z species are EPR-active in both hydrated and dehydrated states, while $[Cu(OH)]^+$-Z species are EPR-active and EPR-silent in hydrated and dehydrated states, respectively, the Cu^{2+} ions in zeolite existing as $[Cu(OH)]^+$-Z and Cu^{2+}-2Z species can be quantified by EPR [22,23,36]. In this work, EPR spectroscopy was used to investigate the changes in EPR-active Cu^{2+} ions, $[Cu(OH)]^+$-Z and Cu^{2+}-2Z species, by comparing the EPR spectra of the hydrated fresh and 920 ºC-aged forms of Cu-LTA catalysts. As shown in Fig. 6, the EPR spectra of all Cu-LTA catalysts in their hydrated form, characterized by the same signal with $g_{||} = 2.355$ and $A_{||} = 149$ G, reveal that the Cu^{2+} ions are located in *s6r* sites [18]. Furthermore, because the signal intensity and line broadening of EPR features are related to the amount of EPR-active

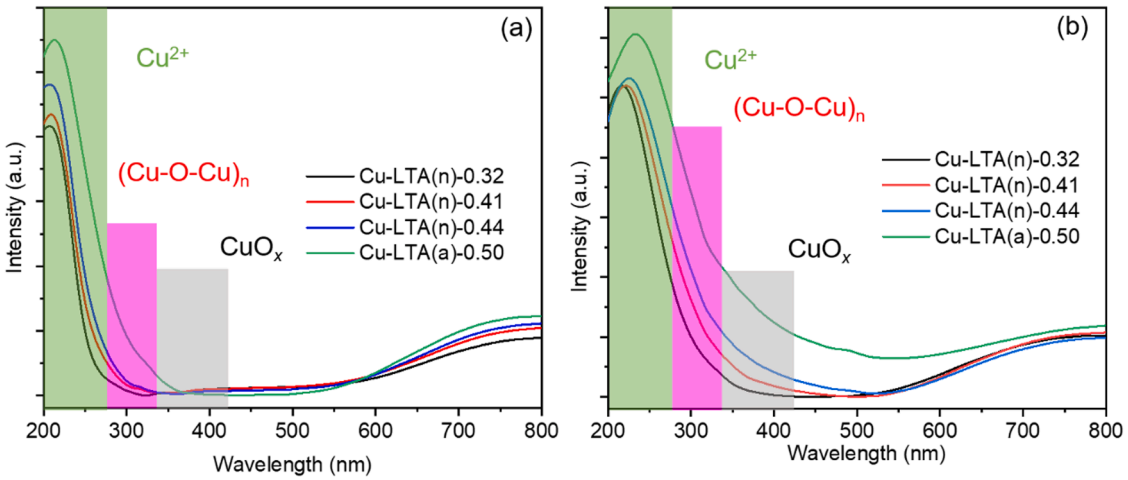

Fig. 4. UV–vis spectra of the (a) fresh and (b) 920 ºC-aged Cu-LTA(n)−0.32, Cu-LTA(n)−0.41, Cu-LTA(n)−0.44, and Cu-LTA(a)−0.50 (from left to right).

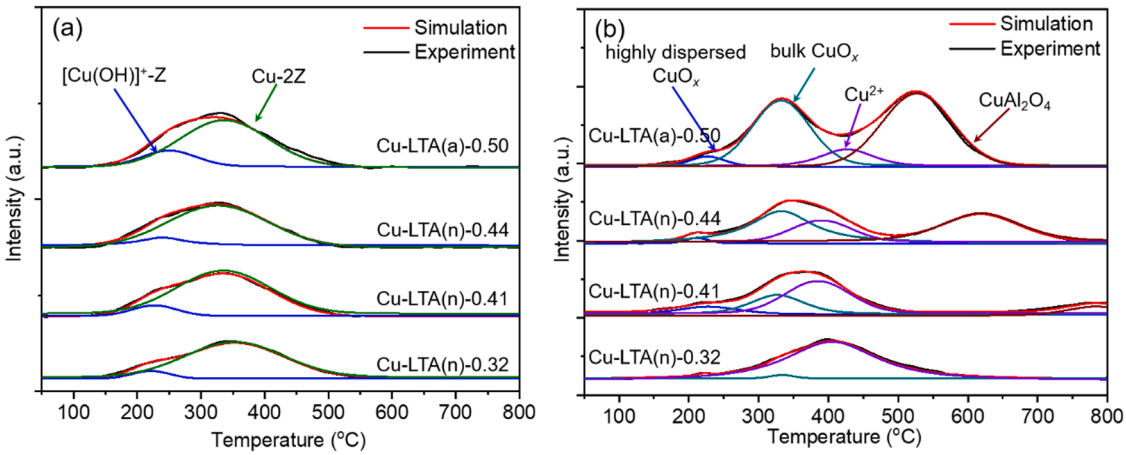

Fig. 5. H_2-TPR profiles of the (a) fresh and (b) 920 °C-aged Cu-LTA(n)−0.32, Cu-LTA(n)−0.41, Cu-LTA(n)−0.44, and Cu-LTA(a)−0.50 (from bottom to top).

Table 2
Populations of different Cu species for Cu-LTA from H_2-TPR results.

catalysts	$[Cu(OH)]^+$-Z[a]	Cu^{2+}-2Z	CuO_x +$CuAl_2O_4$[b]
Cu-LTA(n)−0.32	0.08(0)[c]	0.92(0.98)	0(0.02)
Cu-LTA(n)−0.41	0.10(0)	0.90(0.67)	0(0.33)
Cu-LTA(n)−0.44	0.12(0)	0.88(0.32)	0(0.68)
Cu-LTA(n)−0.50	0.18(0)	0.82(0.18)	0(0.82)

[a] $[Cu(OH)]^+$-Z = 2$[Cu(OH)]^+$-Z/(2$[Cu(OH)]^+$-Z + 2Cu^{2+}-2Z+ CuO_x + $CuAl_2O_4$).
[b] CuO_x + $CuAl_2O_4$ = (CuO_x + $CuAl_2O_4$)/(2$[Cu(OH)]^+$-Z + 2Cu^{2+}-2Z+ CuO_x + $CuAl_2O_4$).
[c] The values in parentheses are the distributions of different copper species in aged Cu-LTA zeolites at 920 °C for 24 h.

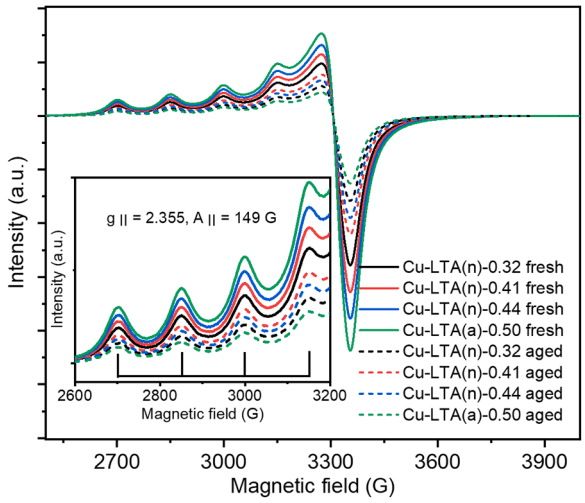

Fig. 6. EPR spectra of fresh and 920 °C-aged Cu-LTA(n)−0.32, Cu-LTA(n)−0.41, Cu-LTA(n)−0.44, and Cu-LTA(a)−0.50. The inset shows an enlargement of the hyperfine region of the EPR spectra.

Cu^{2+} ions, the EPR signal intensities of fresh Cu-LTA catalysts have the same trend as the Cu loadings. The signal intensities decrease in the following order: Cu-LTA(a)−0.50(fresh) > Cu-LTA(n)−0.44(fresh) > Cu-LTA(n)−0.41(fresh) > Cu-LTA(n)−0.32(fresh) > Cu-LTA(n)−0.41(aged) > Cu-LTA(n)−0.44(aged) > Cu-LTA(n)−0.32(aged) > Cu-LTA(a)−0.50(aged). The order of the variation in the amount of EPR-active Cu^{2+} ions in Cu-LTA catalysts coincides well with the low-temperature deNO$_x$ activity (150–300 °C). This provides evidence that the decrease in signal intensities is owing to the transformation of EPR-active Cu^{2+} ions to EPR-silent CuO_x species and $CuAl_2O_4$, resulting in the loss of deNO$_x$ active and the collapse of the LTA structure.

^{27}Al solid-state NMR was conducted to investigate the changes in the coordination status of Al in Cu-LTA catalysts during the hydrothermal aging treatment, and the corresponding ^{27}Al solid-state NMR spectra are presented in Fig. 7. For the fresh catalysts, a single peak centered at ~53 ppm was observed, which is attributed to tetrahedral Al in the zeolite framework. For the Cu-LTA(a)−0.50 catalyst, peaks for five- and six-coordinated extra-framework Al at ~35 and ~− 5 ppm, respectively, were detected after hydrothermal aging treatment. This indicates the conversion of tetrahedral aluminum in the LTA framework to other Al species. Moreover, the broad peak at 53 ppm possibly resulted from another four-coordinated Al [50]. Intriguingly, it was noted that hydrothermal aging only led to partial dealumination for the catalysts with the ratio of Cu/Al < Al_{pair}/Al (Co/Al), and the zeolite structure and deNO$_x$ activity was still maintained, which can be confirmed from the SCR performance, XRD, and BET results. However, hydrothermal aging not only led to dealumination for catalysts with the ratio of Cu/Al > Al_{pair}/Al (Co/Al), but also decreased the deNO$_x$ activity and destroyed the zeolite structure. Taken together, these results demonstrate that the optimum amount of Cu loading in LTA suppresses dealumination and the formation of CuO_x species, as well as maintaining excellent deNO$_x$ activity and structural integrity.

To further investigate the structural integrity of Cu-LTA catalysts, SEM images were recorded. As shown in Fig. 8, all of the samples show a cubic morphology typical of the LTA structure, and the surface of the particles is still smooth. This result suggests that the framework collapse in the aged Cu-LTA(a)−0.50 catalyst occurred in the inner space of LTA. Thus, the high-silica LTA zeolite maintained its basic structure after harsh hydrothermal aging treatment at 920 °C.

To further verify the changes in the physical nature of Cu-LTA catalysts, TEM images of fresh and aged Cu-LTA catalysts are shown in Fig. 9. No discernable particles can be seen in the images of the fresh Cu-LTA catalysts, which means that the Cu species were highly dispersed. After hydrothermal aging at 920 °C for 24 h, many black particles can be observed over the Cu-LTA(a)−0.50 catalyst. This result indicates the conversion of Cu^{2+} ions to CuO_x during the hydrothermal aging treatment, thus leading to the loss of deNO$_x$ activity. However, the structural integrity of the Cu-LTA(a)−0.50 catalyst is still good according to the TEM image. Combining the XRD, BET, and TEM results, the collapse of the Cu-LTA(a)−0.50 catalyst appears to have occurred in the inner spaces of LTA, which is in good agreement with the SEM images. The black particles in the aged Cu-LTA(n)−0.41 and Cu-LTA(n)−0.44 catalysts are quite small, compared with those of the aged Cu-LTA(a)−0.50 catalyst. In addition, it is hard to find CuO_x in the aged Cu-LTA(n)−0.32 catalyst.

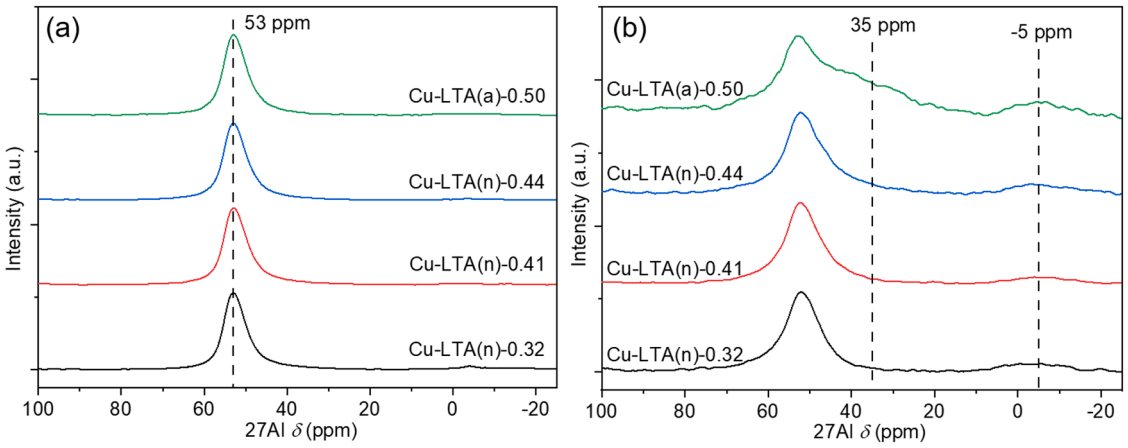

Fig. 7. ^{27}Al solid-state NMR spectra of (a) fresh and (b) 920 ºC-aged Cu-LTA(n)−0.32, Cu-LTA(n)−0.41, Cu-LTA(n)−0.44, and Cu-LTA(a)−0.50 (from bottom to top).

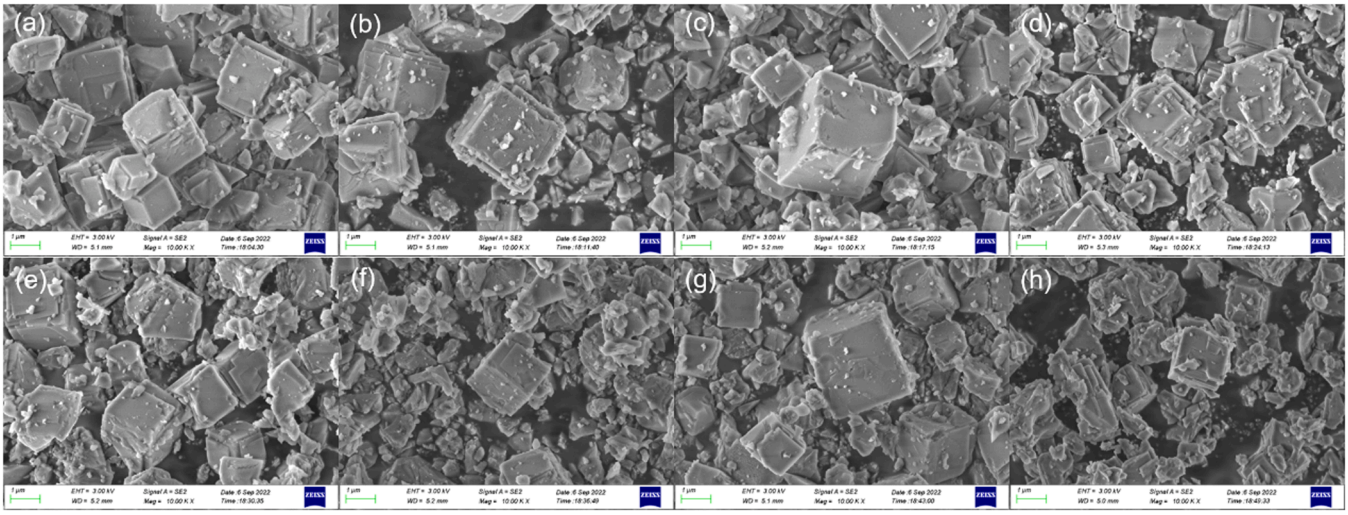

Fig. 8. SEM images of fresh and 920 ºC-aged Cu-LTA catalysts. Cu-LTA(n)−0.32: (a), (e); Cu-LTA(n)−0.41: (b), (f); Cu-LTA(n)−0.44: (c), (g); and Cu-LTA(a)−0.50: (d), (h) All images were collected at 1000 X magnification.

4. Conclusions

A series of Cu-exchanged LTA catalysts for the NH_3-SCR reaction were prepared with various Cu contents (Cu/Al = 0.32–0.5). The fresh Cu-LTA catalysts prepared in this work with higher Cu loadings exhibited better low-temperature ($\leq$ 300 °C) deNO_x activity. After hydrothermal aging at 920 °C for 24 h, the fully Cu-exchanged LTA catalyst, Cu-LTA(a)−0.50, almost completely lost its deNO_x activity, whereas the Cu-LTA(n)−0.41 catalyst maintained its deNO_x activity and zeolite structure well. Those results suggest that optimizing the Cu loading can significantly enhance the hydrothermal stability of the Cu-LTA catalysts. It is well-accepted that more Cu^{2+}-2Z species in Cu-exchanged zeolite catalysts can improve their hydrothermal durability, since the Cu^{2+}-2Z species are more hydrothermally stable than $[Cu(OH)]^+$-Z species. Furthermore, the formation of CuO_x and $CuAl_2O_4$ from the conversion of $[Cu(OH)]^+$-Z species during hydrothermal aging treatment is the primary reason for deactivation and structure collapse. Reducing the amount of less-stable $[Cu(OH)]^+$-Z species will be an effective strategy for designing catalysts with excellent deNO_x activity and hydrothermal stability. For the Cu-LTA(n)−0.41 catalyst, the optimal Cu content is beneficial in two ways. First, introducing high Cu content to provide high deNO_x activity; second, suppressing the formation of unstable $[Cu(OH)]^+$-Z species to maintain high hydrothermal stability. Combining the results of multiple characterization methods, such as XRD, BET, H_2-TPR NMR, UV–vis, and EPR, it is concluded that optimizing the Cu loading and controlling its location are the key reasons the obtained Cu-LTA(n)−0.41 catalyst (with maximum amount and ratio of Cu^{2+}-2Z species) can endure hydrothermal aging under the extremely harsh conditions of 920 °C for 24 h. We believe this to be a breakthrough in the pursuit of NH_3-SCR catalysts with higher hydrothermal stability.

CRediT authorship contribution statement

Jinhan Lin: Investigation, Conceptualization, Writing – original draft, Writing – review & editing. **Xueyang Hu:** Data curation, Writing – review & editing. **Yingjie Li:** Data curation, Writing – review & editing. **Xuechao Tan:** Conceptualization, Writing – review & editing. **Wenpo Shan:** Resources, Supervision, Writing – review & editing, Project administration, Funding acquisition. **Hong He:** Resources, Supervision, Funding acquisition, Writing – review & editing.

Declaration of Competing Interest

The authors declare that they have no known competing financial interests or personal relationships that could have appeared to influence the work reported in this paper.

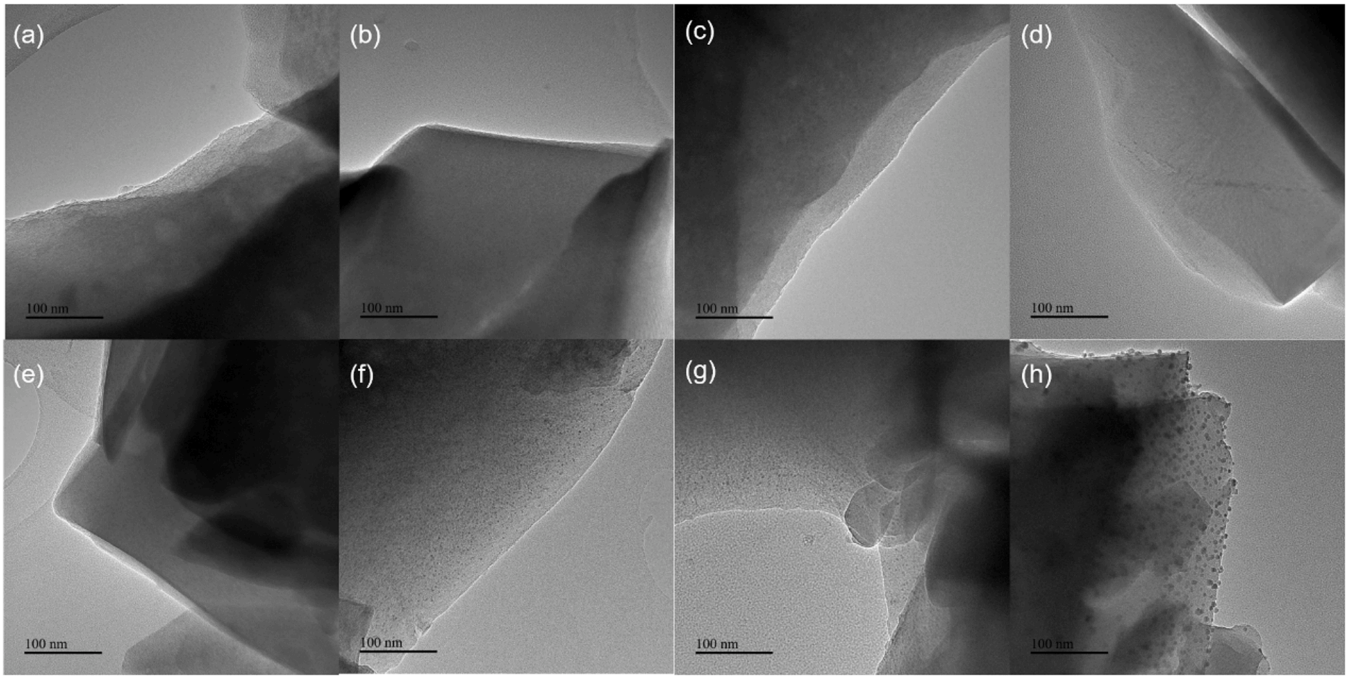

Fig. 9. TEM images of fresh and 920 °C-aged Cu-LTA catalysts. Cu-LTA(n)−0.32: (a), (e); Cu-LTA(n)−0.41: (b), (f); Cu-LTA(n)−0.44: (c), (g); and Cu-LTA(a)−0.50: (d), (h). All images were collected at 120 kX magnification.

Data availability

Data will be made available on request.

Acknowledgments

This work was financially supported by the National Natural Science Foundation of China (52225004, 51978640), the National Key R&D Program of China (2022YFC3701804), and the Science and Technology Innovation "2025" Major Program in Ningbo (2020Z103). We would also like to acknowledge Prof. Suk Bong Hong at Pohang University of Science and Technology (POSTECH) for his kind and patient guidance in the preparation of Cu-LTA.

Appendix A. Supplementary material

Supplementary data associated with this article can be found in the online version at doi:10.1016/j.apcatb.2023.122705.

References

[1] R. Zhang, N. Liu, Z. Lei, B. Chen, Selective transformation of various nitrogen-containing exhaust gases toward N_2 over zeolite catalysts, Chem. Rev. 116 (2016) 3658–3721.
[2] J. Wang, H. Zhao, G. Haller, Y. Li, Recent advances in the selective catalytic reduction of NO_x with NH_3 on Cu-Chabazite catalysts, Appl. Catal. B Environ. 202 (2017) 346–354.
[3] L. Han, S. Cai, M. Gao, J.Y. Hasegawa, P. Wang, J. Zhang, L. Shi, D. Zhang, Selective catalytic reduction of NO_x with NH_3 by using novel catalysts: state of the art and future prospects, Chem. Rev. 119 (2019) 10916–10976.
[4] Y. Shan, J. Du, Y. Zhang, W. Shan, X. Shi, Y. Yu, R. Zhang, X. Meng, F.S. Xiao, H. He, Selective catalytic reduction of NO_x with NH_3: opportunities and challenges of Cu-based small-pore zeolites, Natl. Sci. Rev. 8 (2021) nwab010.
[5] S. Mohan, P. Dinesha, S. Kumar, NO_x reduction behaviour in copper zeolite catalysts for ammonia SCR systems: a review, Chem. Eng. J. 384 (2020) 123253–123262.
[6] F. Liu, Y. Yu, H. He, Environmentally-benign catalysts for the selective catalytic reduction of NO_x from diesel engines: structure-activity relationship and reaction mechanism aspects, Chem. Commun. 50 (2014) 8445–8463.
[7] Y. Xin, Q. Li, Z.L. Zhang, Zeolitic materials for deNO_x selective catalytic reduction, ChemCatChem 10 (2018) 29–41.
[8] Y. Ma, H. Zhao, C. Zhang, Y. Zhao, H. Chen, Y. Li, Enhanced hydrothermal stability of Cu-SSZ-13 by compositing with Cu-SAPO-34 in selective catalytic reduction of nitrogen oxides with ammonia, Catal. Today 355 (2020) 627–634.
[9] L. Ma, Y. Cheng, G. Cavataio, R.W. McCabe, L. Fu, J. Li, Characterization of commercial Cu-SSZ-13 and Cu-SAPO-34 catalysts with hydrothermal treatment for NH_3-SCR of NO_x in diesel exhaust, Chem. Eng. J. 225 (2013) 323–330.
[10] K. Zha, L. Kang, C. Feng, L. Han, H. Li, T. Yan, P. Maitarad, L. Shi, D. Zhang, Improved NO_x reduction in the presence of alkali metals by using hollandite Mn–Ti oxide promoted Cu-SAPO-34 catalysts, Environ. Sci. Nano 5 (2018) 1408–1419.
[11] L. Yan, Y. Ji, P. Wang, C. Feng, L. Han, H. Li, T. Yan, L. Shi, D. Zhang, Alkali and phosphorus resistant zeolite-like catalysts for NO_x reduction by NH_3, Environ. Sci. Technol. 54 (2020) 9132–9141.
[12] P. Wang, L. Yan, Y. Gu, S. Kuboon, H. Li, T. Yan, L. Shi, D. Zhang, Poisoning-resistant NO_x reduction in the presence of alkaline and heavy metals over H-SAPO-34-supported Ce-promoted Cu-based catalysts, Environ. Sci. Technol. 54 (2020) 6396–6405.
[13] J. He, S. Impeng, J. Zhang, J. Zhang, P. Wang, D. Zhang, SO_2-tolerant NO_x reduction over SO_4^{2-}-coordinated Cu-SAPO-34 catalysts via protecting the reduction and re-oxidation of Cu sites, Chem. Eng. J. 448 (2022) 137720–137728.
[14] Y. Zhang, H. Zhu, T. Zhang, J. Li, J. Chen, Y. Peng, J. Li, Revealing the synergistic deactivation mechanism of hydrothermal aging and SO_2 poisoning on Cu/SSZ-13 under SCR condition, Environ. Sci. Technol. 56 (2022) 1917–1926.
[15] S.J. Schmieg, S.H. Oh, C.H. Kim, D.B. Brown, J.H. Lee, C.H.F. Peden, D.H. Kim, Thermal durability of Cu-CHA NH_3-SCR catalysts for diesel NO_x reduction, Catal. Today 184 (2012) 252–261.
[16] U. Deka, I. Lezcano-Gonzalez, B.M. Weckhuysen, A.M. Beale, Local environment and nature of Cu active sites in zeolite-based catalysts for the selective catalytic reduction of NO_x, ACS Catal. 3 (2013) 413–427.
[17] T. Ryu, H. Kim, S.B. Hong, Nature of active sites in Cu-LTA NH_3-SCR catalysts: a comparative study with Cu-SSZ-13, Appl. Catal. B Environ. 245 (2019) 513–521.
[18] T. Ryu, N.H. Ahn, S. Seo, J. Cho, H. Kim, D. Jo, G.T. Park, P.S. Kim, C.H. Kim, E. L. Bruce, P.A. Wright, I.S. Nam, S.B. Hong, Fully copper-exchanged high-silica LTA zeolites as unrivaled hydrothermally stable NH_3-SCR catalysts, Angew. Chem. Int. Ed. 56 (2017) 3256–3260.
[19] D. Jo, T. Ryu, G.T. Park, P.S. Kim, C.H. Kim, I.S. Nam, S.B. Hong, Synthesis of high-silica LTA and UFI zeolites and NH_3-SCR performance of their copper-exchanged form, ACS Catal. 6 (2016) 2443–2447.
[20] N.H. Ahn, T. Ryu, Y. Kang, H. Kim, J. Shin, I.S. Nam, S.B. Hong, The origin of an unexpected increase in NH_3-SCR activity of aged Cu-LTA catalysts, ACS Catal. 7 (2017) 6781–6785.
[21] J. Lin, K. Lee, S.B. Hong, Effect of preparation method on NH_3-SCR activity of Cu-LTA catalysts, Catal. Today 376 (2021) 41–46.
[22] F. Gao, J. Szanyi, On the hydrothermal stability of Cu/SSZ-13 SCR catalysts, Appl. Catal. A Gen. 560 (2018) 185–194.
[23] J. Song, Y. Wang, E.D. Walter, N.M. Washton, D. Mei, L. Kovarik, M.H. Engelhard, S. Prodinger, Y. Wang, C.H.F. Peden, F. Gao, Toward rational design of Cu/SSZ-13 selective catalytic reduction catalysts: Implications from atomic-level understanding of hydrothermal stability, ACS Catal. 7 (2017) 8214–8227.

[24] Y. Shan, W. Shan, X. Shi, J. Du, Y. Yu, H. He, A comparative study of the activity and hydrothermal stability of Al-rich Cu-SSZ-39 and Cu-SSZ-13, Appl. Catal. B Environ. 264 (2020) 118511–118520.
[25] J. Zhang, Y. Shan, L. Zhang, J. Du, H. He, S. Han, C. Lei, S. Wang, W. Fan, Z. Feng, X. Liu, X. Meng, F.-S. Xiao, Importance of controllable Al sites in CHA framework by crystallization pathways for NH_3-SCR reaction, Appl. Catal. B Environ. 277 (2020) 119193–119200.
[26] A. Guo, K. Xie, H. Lei, V. Rizzotto, L. Chen, M. Fu, P. Chen, Y. Peng, D. Ye, U. Simon, Inhibition effect of phosphorus poisoning on the dynamics and redox of Cu active sites in a Cu-SSZ-13 NH_3-SCR catalyst for NO_x reduction, Environ. Sci. Technol. 55 (2021) 12619–12629.
[27] A. Wang, L. Olsson, Insight into the SO_2 poisoning mechanism for NO_x removal by NH_3-SCR over Cu/LTA and Cu/SSZ-13, Chem. Eng. J. 395 (2020) 125048–125060.
[28] R. Yu, H. Kong, Z. Zhao, C. Shi, X. Meng, F.S. Xiao, T. De Baerdemaeker, A. N. Parvulescu, U. Müller, W. Zhang, Rare-earth yttrium exchanged Cu-SSZ-39 zeolite with superior hydrothermal stability and SO_2 -tolerance in NH_3-SCR of NO_x, ChemCatChem 14 (2022).
[29] Z. Chen, T. Ye, H. Qu, T. Zhu, Q. Zhong, Progressive regulation of Al sites and Cu distribution to increase hydrothermal stability of hierarchical SSZ-13 for the selective catalytic reduction reaction, Appl. Catal. B Environ. 303 (2022) 120867–120877.
[30] Q. Lin, S. Xu, H. Zhao, S. Liu, H. Xu, Y. Dan, Y. Chen, Highlights on key roles of Y on the hydrothermal stability at 900 °C of Cu/SSZ-39 for NH3-SCR, ACS Catal. 12 (2022) 14026–14039.
[31] J. Dědeček, B. Wichterlová, Role of hydrated Cu ion complexes and aluminum distribution in the framework on the Cu ion siting in ZSM-5, J. Phys. Chem. B 101 (1997) 10233–10240.
[32] A. Itadani, Y. Kuroda, M. Nagao, Elucidation of a preparation method for copper ion-exchanged ZSM-5 samples exhibiting extremely efficient N_2-adsorption at room temperature: effect of counter ions in the exchange solution, Microporous Mesoporous Mater. 70 (2004) 119–126.
[33] S. Zhou, F. Tang, H. Wang, S. Wang, L. Liu, Effect of Cu concentration on the selective catalytic reduction of NO with ammonia for aluminosilicate zeolite SSZ-13 catalysts, J. Phys. Chem. C 125 (2021) 14675–14680.
[34] Y. Shan, X. Shi, G. He, K. Liu, Z. Yan, Y. Yu, H. He, Effects of NO_2 addition on the NH_3-SCR over small-pore Cu–SSZ-13 zeolites with varying Cu loadings, J. Phys. Chem. C 122 (2018) 25948–25953.
[35] D. Yao, B. Liu, F. Wu, Y. Li, X. Hu, W. Jin, X. Wang, N_2O formation mechanism during low-temperature NH_3-SCR over Cu-SSZ-13 catalysts with different Cu loadings, Ind. Eng. Chem. Res. 60 (2021) 10083–10093.
[36] F. Gao, E.D. Walter, E.M. Karp, J.Y. Luo, R.G. Tonkyn, J.H. Kwak, J. Szanyi, C.H. F. Peden, Structure-activity relationships in NH_3-SCR over Cu-SSZ-13 as probed by reaction kinetics and EPR studies, J. Catal. 300 (2013) 20–29.
[37] X. Wei, Q. Ke, H. Cheng, Y. Guo, Z. Yuan, S. Zhao, T. Sun, S. Wang, Seed-assisted synthesis of Cu-(Mn)-UZM-9 zeolite as excellent NO removal and N_2O inhibition catalysts in wider temperature window, Chem. Eng. J. 391 (2020).
[38] C. Paolucci, A.A. Parekh, I. Khurana, J.R. Di Iorio, H. Li, J.D. Albarracin Caballero, A.J. Shih, T. Anggara, W.N. Delgass, J.T. Miller, F.H. Ribeiro, R. Gounder, W. F. Schneider, Catalysis in a cage: condition-dependent speciation and dynamics of exchanged Cu cations in SSZ-13 zeolites, J. Am. Chem. Soc. 138 (2016) 6028–6048.
[39] J. Dedecek, E. Tabor, S. Sklenak, Tuning the aluminum distribution in zeolites to increase their performance in acid-catalyzed reactions, ChemSusChem 12 (2019) 556–576.
[40] Z. Chen, C. Fan, L. Pang, S. Ming, P. Liu, T. Li, The influence of phosphorus on the catalytic properties, durability, sulfur resistance and kinetics of Cu-SSZ-13 for NO_x reduction by NH_3 -SCR, Appl. Catal. B Environ. 237 (2018) 116–127.
[41] C. Fan, Z. Chen, L. Pang, S. Ming, X. Zhang, K.B. Albert, P. Liu, H. Chen, T. Li, The influence of Si/Al ratio on the catalytic property and hydrothermal stability of Cu-SSZ-13 catalysts for NH_3-SCR, Appl. Catal. A Gen. 550 (2018) 256–265.
[42] H. Zhao, X. Wu, Z. Huang, Z. Chen, G. Jing, A comparative study of the thermal and hydrothermal aging effect on Cu-SSZ-13 for the selective catalytic reduction of NO with NH_3, Chin. J. Chem. Eng. 45 (2022) 68–77.
[43] H. Zhao, Y. Zhao, M. Liu, X. Li, Y. Ma, X. Yong, H. Chen, Y. Li, Phosphorus modification to improve the hydrothermal stability of a Cu-SSZ-13 catalyst for selective reduction of NO_x with NH_3, Appl. Catal. B Environ. 252 (2019) 230–239.
[44] J. Luo, F. Gao, K. Kamasamudram, N. Currier, C.H.F. Peden, A. Yezerets, New insights into Cu/SSZ-13 SCR catalyst acidity. Part I: nature of acidic sites probed by NH_3 titration, J. Catal. 348 (2017) 291–299.
[45] J.H. Lee, Y.J. Kim, T. Ryu, P.S. Kim, C.H. Kim, S.B. Hong, Synthesis of zeolite UZM-35 and catalytic properties of copper-exchanged UZM-35 for ammonia selective catalytic reduction, Appl. Catal. B Environ. 200 (2017) 428–438.
[46] D. Jo, G.T. Park, T. Ryu, S.B. Hong, Economical synthesis of high-silica LTA zeolites: a step forward in developing a new commercial NH_3-SCR catalyst, Appl. Catal. B Environ. 243 (2019) 212–219.
[47] Z. Chen, C. Fan, L. Pang, S. Ming, P. Liu, D. Zhu, J. Wang, X. Cai, H. Chen, Y. Lai, T. Li, Direct synthesis of submicron Cu-SAPO-34 as highly efficient and robust catalyst for selective catalytic reduction of NO by NH_3, Appl. Surf. Sci. 448 (2018) 671–680.
[48] A. Wang, P. Arora, D. Bernin, A. Kumar, K. Kamasamudram, L. Olsson, Investigation of the robust hydrothermal stability of Cu/LTA for NH_3-SCR reaction, Appl. Catal. B Environ. 246 (2019) 242–253.
[49] M.-F. Luo, P. Fang, M. He, Y.-L. Xie, In situ XRD, Raman, and TPR studies of CuO/Al_2O_3 catalysts for CO oxidation, J. Mol. Catal. A Chem. 239 (2005) 243–248.
[50] Z. Zhao, R. Yu, R. Zhao, C. Shi, H. Gies, F.-S. Xiao, D. De Vos, T. Yokoi, X. Bao, U. Kolb, M. Feyen, R. McGuire, S. Maurer, A. Moini, U. Müller, W. Zhang, Cu-exchanged Al-rich SSZ-13 zeolite from organotemplate-free synthesis as NH_3-SCR catalyst: effects of Na^+ ions on the activity and hydrothermal stability, Appl. Catal. B Environ. 217 (2017) 421–428.